Waste Biomass Valor
DOI 10.1007/s12649-016-9814-8

ORIGINAL PAPER

Selection of Biorefinery Routes: The Case of Xylitol and its Integration with an Organosolv Process

A. D. Mountraki[1,2] · K. R. Koutsospyros[2] · B. Benjelloun Mlayah[1] · A. C. Kokossis[2]

Received: 30 June 2016 / Accepted: 20 December 2016

Abstract Lignocellulosic biomass includes agricultural and forest residues, which is a promising source for energy and chemical production when valorized through the biorefinery process. Xylitol is an important co-product in biorefinery. The production of xylitol is achieved either by yeast fermentation or by catalytic hydrogenation of xylose. However these approaches are not viable unless integrated. This paper presents a comparative analysis and the integrating opportunities of two processes for the production of xylitol, assessing the scope for individual integration as well as integration with upstream and parallel processes. The two processes examined are the fermentation of xylose by Candida yeasts (productivity 0.73 kg xylitol crystals/kg xylose), and the catalytic hydrogenation of xylose using a Raney Nickel catalyst (productivity 0.85 kg xylitol crystals/kg xylose). The heat integration analysis resulted in conservation of 90% for cooling and 18% for heating requirements in the catalytic process. The corresponding results in the biotechnological process were 94 and 65% respectively. The economic evaluation estimated higher total investment and raw materials-utilities cost for the biotechnological process in comparison to the catalytic by 391 and 8% respectively. The economic indexes characterize the catalytic process investment as more secure and profitable.

Keywords Xylitol · Process design · Cost estimation · Integration · Biorefinery

✉ A. D. Mountraki
a.mountraki@cimv.fr; mountrak@central.ntua.gr

[1] Compagnie Industrielle de la Matière Végétale (CIMV), 109 rue Jean Bart - Diapason A, 31670 Toulouse, France

[2] National Technical University of Athens (NTUA), 9 Heroon Politechniou, Politechnioupoli, Zografos 15780, Greece

Abbreviations

C5	Pentoses (five carbon sugars)
C6	Hexoses (six carbon sugars)
CEPCI	Chemical engineering plant cost index
CIMV	Compagnie Industrielle de la Matière Végétale (tr. industrial company of vegetative material)
cr	Crystallized
GCC	Grand composite curves
LHV	Lower heating value
MILP	Mixed integer linear programming
MINLP	Mixed integer non linear programming
MM	Million
NPV	Net present value
PBP	Payback period
USD	United states dollar

Introduction

Biorefineries account for the most efficient valorization of lignocellulosic residue; however, they should build efficiency with process integration in order to remain competitive to the chemical industry. The latter relates to the efficient use of energy [1–3], water [4–8], and process flowsheeting [9, 10]. There are numerous options for producing fuels and chemicals from biomass through thermochemical or biochemical paths. The integration of a particular path, either within itself or with respect to the background processes available, improves the process efficiencies making its selection attractive. The selection spans different types of feedstock, reaction yields, and technologies. In each case, one is required to review a large number of production paths with respect to economic objectives and environmental criteria [11]. A systematic framework has been proposed as a three layer approach that includes

Published online: 27 January 2017

flowsheeting, integration and synthesis [12–14]. The approach is summarized in Fig. 1 and includes:

Synthesis to screen products and paths,

Process Integration to target performance with respect to raw material and energy use, and

Process Flowsheeting for modeling at different levels to evaluate the level of uncertainty in feedstock composition, process chemistries, and costs.

Synthesis identifies promising (viable, economic, sustainable) routes, while process integration establishes performance targets to enable comparisons justifying recommendations over seemingly equal choices. Flowsheeting provides a reference basis for mass and energy balances, as well as the background to validate the choices recommended by synthesis and integration. The search initiates at the lower layer (flowsheeting), iterating through synthesis and integration. Synthesis offers new candidates to expand and improve the sustainability of the initial stage; process and energy integration evaluates candidates and validates the proposed integrated schemes, essentially turning the workflow back to flowsheeting. Iterations continue unless a set of selected of economic and environmental criteria are satisfied.

The use of the systems framework of Fig. 1 has been applied extensively to develop biorefinery designs and has demonstrated that xylitol can strongly vindicate its place amongst biorefinery value chain products [9, 15–20].

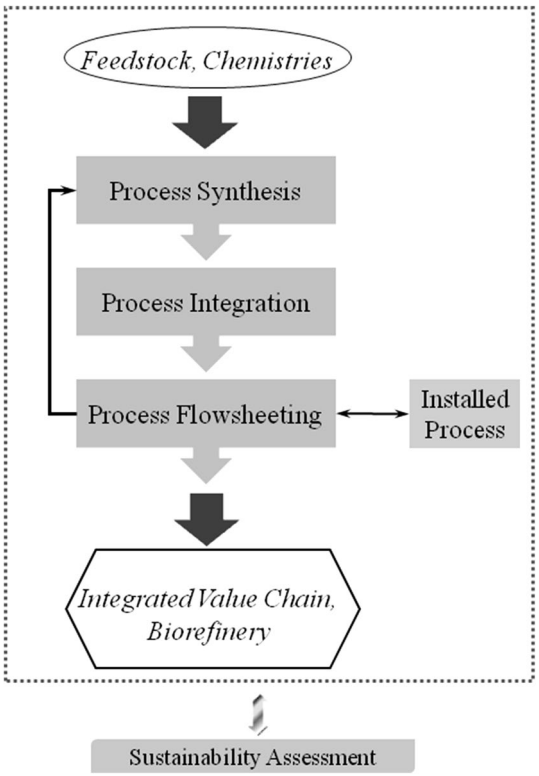

Fig. 1 The three layer approach

Current work addresses a real-life biorefinery [21] featuring three main products (cellulose, hemi-cellulose, and lignin). It is possible to valorize these products by making use of the paths of Fig. 2. Tsakalova and coworkers [19, 22] have studied the general problem of selecting paths and products from multiple feedstocks. Their synthesis stage has been applied already to assess promising chemistries, ranking and valorizing the different products both economically (profits, costs) and environmentally. Indeed, their approach reviewed products and paths considering.

- The unrestricted set of products on the basis of nominal (fixed) prices and maximum demands;
- Different sets of constraints on demands, prices and processing parameters as they have been dictated by practitioners.

The results of the synthesis models are certainly consistent with the growing demand for sugar-free and low-calorie food products have attracted the attention of xylitol production from hemicelluloses [23–25]. Xylitol is a substance of great commercial value as a food additive, with a lot of health benefits [26–28]. Its share in the global market is expected to reach 242,000 metric tons valued at just above US$1 billion by 2020 [29], making it an important co-product in biorefinery. Xylitol valorizes the fraction of pentoses (C5) of hydrolyzed biomass and is entirely complementary to the production of bioethanol from hexoses (C6) [30].

Even though xylitol emerges as a promising chemical, the results of synthesis stand only as a preliminary indication for a promising option. Important decisions are left to be made before the selection is confirmed. As they should, synthesis models rely on gross material and energy balances available from process flowsheets; no further details are transferred to the synthesis models. The remaining stages (integration, flowsheeting) are required to take the analysis deeper and to clarify the actual scope in producing the product. The systems approach of Fig. 1 advocates that the use of simulation and flowsheeting is still inappropriate; some higher-level analysis is required instead. In view of the additional decisions in mind, one then is left to address:

- If not a flowsheet model, what is the process representation to deploy by the analysis?
- Other than the economics (that are considered already), what is the basis to select production technologies for xylitol?
- What is the scope to integrate candidate technology with its background process (e.g. production of intermediates)?

This paper explains these challenges in the background of a promising organoslov technology, the CIMV Process™.

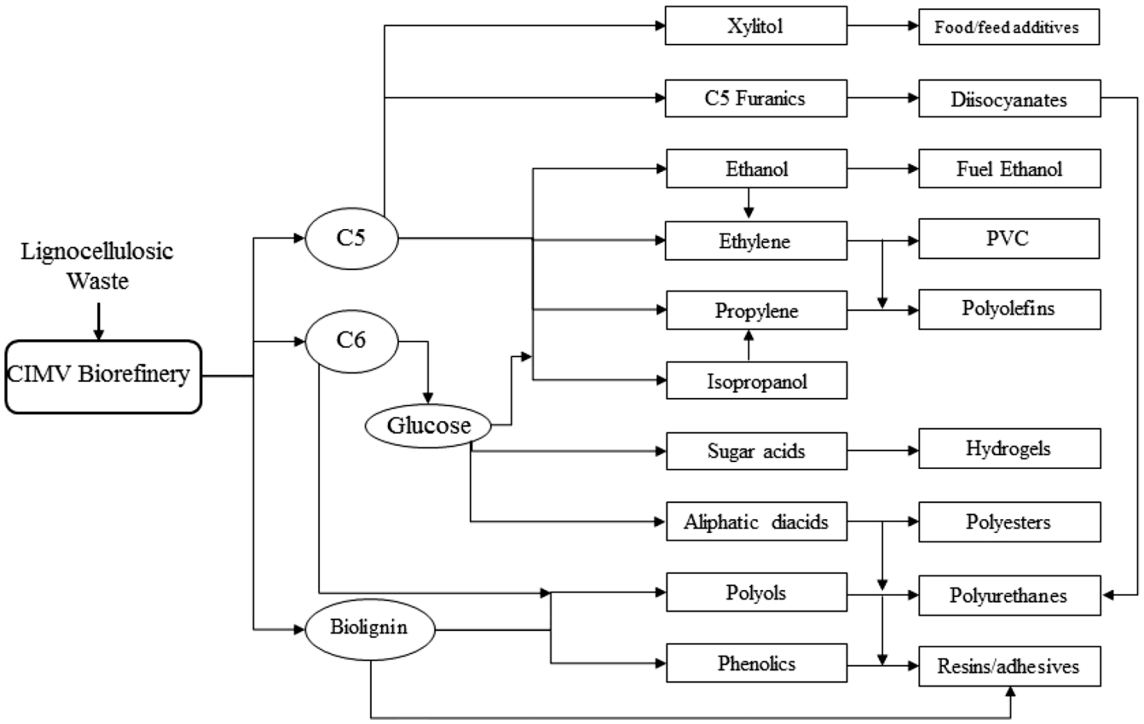

Fig. 2 Value chain of a lignocellulosic biorefinery

CIMV (Compagnie Industrielle de la Matière Végétale—industrial company of vegetative material) organosolv technology operates a lignocellulosic biorefinery process. Biomass undertakes an extraction stage through which lignin and hemicellulose fragments are dissolved in organic acids (formic and acetic acid). Lignin and soluble sugars are separated after lignin precipitation. Soluble C5 sugars are obtained in a form of syrup, after concentration, while lignin is filtered, washed, and dried. The cellulosic pulp obtained undergoes a delignification stage. The final products are Biolignin™ as a phenolic oligomer with a linear and a low molecular weight, cellulosic pulp, which can be hydrolyzed into glucose, and sugars syrup that is mainly composed of monomers of xylose. The C5 syrup product can be further enzymatically hydrolyzed into xylose [31]. The CIMV technology is applicable to a wide range of feedstock including cereal straws, sugarcane bagasse, sweet sorghum bagasse, and softwood. Its major advantage is that the technology separates the biomass fractions without degradation of the celluloses, hemicelluloses, and lignin [32]. The biorefinery paths that could spring from the CIMV intermediates offer an impressive list of chemicals, biofuels, food and feed components, fibers, and energy products. Current work considers the production of two economically competitive paths to xylitol, namely a catalytic process and a biochemical process. Biochemical production of xylitol is a batch or semi-batch process. The choice has to be made considering each process separately but also in relation to the background set by other intermediates in the CIMV value chain. The integration models make use of graphical tools (grand composite curves (GCC), total site profiles, hardware composites) [33–35]. It should be reminded that graphical tools could occasionally be replaced by mathematical formulations in the form of mixed integer linear programming (MILP) or - mixed integer non linear programming (MINLP) models [36, 37] that automate and generalize the analysis (or prepare for high-throughput functions).

At first, the design of two different technologies is reviewed and compared: the catalytic and the biochemical production of xylitol, emphasizing on the process development and the main production stages for each production path. Then, we examine the problem representation that is required to review the scope for integration. Process integration is considered separately for each production path as well as with respect to the background processes (process-to-process integration). Finally, the two processes are economically evaluated.

Process Design

The process design for the production of xylitol has been discussed in a previous work [38]. Both, catalytic and biochemical processes consist of three major sections, namely:

1. Pretreatment section
2. Reaction— Condensation section
3. Crystallization section

The hydrolyzed C5 sugar syrup product of CIMV is used as feed and contains 60% xylose, 30% water, 5% pentoses, 3% acetic acid, and 2% of other chemical impurities (formic acid, lignin, soluble, and insoluble components). The pretreatment removes substances that inhibit or poison the catalyst also regulating the pH. The conversion of xylose to xylitol takes place in the reaction-condensation section, and the water content is regulated before entering the crystallization section. The final product is crystallized as xylitol (cr). The non-random-two-liquid (NRTL) thermodynamic model is used, which can describe vapor–liquid and liquid–liquid equilibrium of highly non-ideal solutions.

Catalytic Process

A schematic block for the process is sketched in Fig. 3. The catalytic hydrogenation of xylose to xylitol takes place at high pressures (40–70 bars) and temperatures (80–140 °C). The residence time in the reactor is 2–3 h, and the catalyst used is Raney Nickel [39].

Figure 4 presents the flow diagram developed in Aspen-Plus. The pretreatment is intended to prepare the reactor feed at optimal conditions. Unit P1 removes 99% of the feed impurities and essentially combines a sequence of treatment stages that use ionic resins, activated carbon column, and chromatographic separation. Unit R1 adjusts the pH in a range of 5–6 through the neutralization of acids by 1 M solution of calcium hydroxide ($Ca(OH)_2$), as shown in reaction 1 (R.1). Before entering the reaction section, unit P2 removes the salt calcium propionate ($Ca(CH_3COO)_2$) [39–41]. The reactor R2 operates at 100 °C and 50 bar. The feed concentration of xylose is 40–60%. The main reaction is the hydrogenation of xylose to xylitol, described by (R.2). The conversion is 95%; higher temperatures favor by-product reactions and the degradation of xylose to furfural. The remaining xylose is converted into xylulose monosaccharide (R.3) that is converted to arabinitol (R.4) at 90% [39–41].

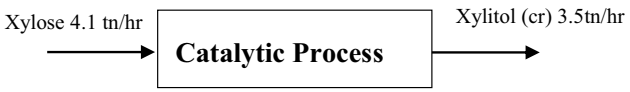

Fig. 3 Conceptual flows for the catalytic xylitol production

Acids neutralization:

$$2C_2H_4O_2 + Ca(OH)_2 \leftrightarrow 2H_2O + Ca(CH_3COO)_2 \quad ((R.1))$$

Xylose to Xylitol:

$$C_5H_{10}O_5 + H_2 \leftrightarrow C_5H_{12}O_5 \quad ((R.2))$$

Xylose to Xylulose:

$$C_5H_{10}O_5 \leftrightarrow C_5H_{10}O_5 \quad ((R.3))$$

Xylulose to Arabinitol:

$$C_5H_{10}O_5 + H_2 \leftrightarrow C_5H_{12}O_5 \quad ((R.4))$$

The catalyst is introduced in a mass ratio of 5% of xylose. The process recycles 95% of the catalyst that is reactivated using alcoholic (mainly ethanol) solutions. The catalyst degrades by the presence of oxygen (air) and survives longer in inert environments.

The product stream (19) is cooled at 80 °C and is subsequently purified using ion exchange membranes and activated carbon columns (units P3 and P4) operating at pH 6–7 for 60 min (or until all contaminants are removed). The purification simultaneously decolours the product and is followed by evaporation (unit EVAP). The xylitol concentration past evaporation is 650–900 g/l [42]. During

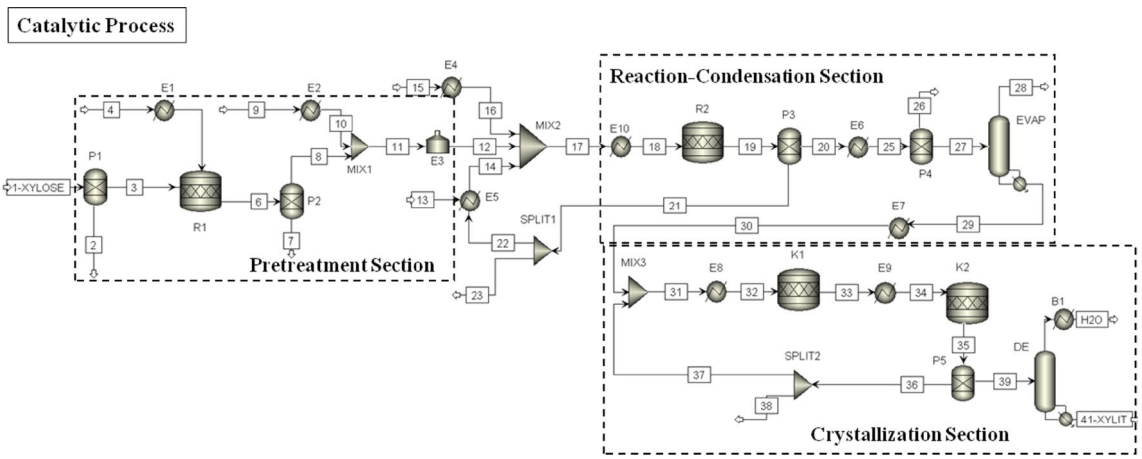

Fig. 4 Aspen flowsheet: Catalytic Xylitol Production

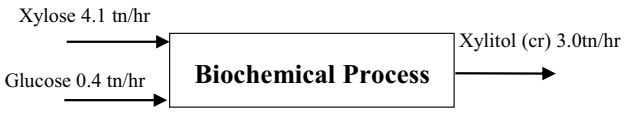

Fig. 5 Conceptual flows for the biochemical xylitol production

the entire process, the temperature remains below 105 °C; otherwise, xylitol degrades to xylose. The latter constraint essentially enforces the evaporator to operate in vacuum. Crystallization follows a two-step process. First, xylitol enters the crystallizer (unit K1), which operates at 8 °C for 24 h. Then, the temperature is further decreased at −20 °C for another 72 h (unit K2). The crystallizers (units K1 & K2) are modeled as stoichiometric reactors, and the yield of xylitol crystal is considered fixed at 0.81 kg xylitol cr/kg xylose, based on data provided by experimental groups. After the crystallization, the xylitol crystals are purified by centrifugation or sedimentation from the mother liquor, and the amount of remaining impurities is significantly decreased by fractionation on parallel ion-exchange columns (unit P5). Finally, the purified crystallized product is dried (DE).

Biochemical Process

A conceptual schematic of the process is shown in Fig. 5. The biochemical yield is 0.73 kg xylitol (cr) (base: 1 kg xylose).

Figure 6 presents the flow diagram developed in Aspen-Plus for the biochemical production of xylitol. The feed is pre-treated as microorganisms are affected by the pH, and the crystallization section follows the same design as in the catalytic process. Contrary to the catalytic method that is favored by concentrated solutions, the biochemical method requires diluted solutions of xylose. The optimal concentration depends on the organism used. In our case (yeast of the genus Candida) the concentration ranges from 50 to 100 g/l. The presence of sugars other than xylose may improve the activity of the microorganism, by improving the cell growth, but it may cause some inhibition effects as well [43, 44]. Hence, glucose is added in a mass ratio of 10% of xylose. Other added nutrients include nitrogen (e.g. NH_3, NH_4OH, NH_4SO_4) and phosphorus (e.g. potassium phosphate). The bioreactor (unit R2) operates at 1 bar and 30 °C under micro-aerobic conditions (0.4–1vvm) with slightly acidic or neutral pH (pH 5–7) [45–47].

The total xylose consumption may reach up to 95%, while the residence time in the bioreactor ranges from 35 to over 100 h [27, 48]. The mild conditions restrict by-products, such as furfurals, that are toxic for the microorganisms [27, 30, 49, 50]. The simulation model is setup to support cost calculations. Reactor R2 is modeled assuming a fixed conversion at 92%. The reactions (R.5) and the metabolic activity of the microorganisms (cell growth and respiration; glucose is assumed to be 100% consumed) (R.6) are given below:

Xylitol Production:

$$100C_5H_{10}O_5 + 8.75O_5 + 7NH_3 + 37H_2 \leftrightarrow 35CH_{1.8}O_{0.5}N_{0.2} + 35CO_2 + 86C_5H_{12}O_5 \quad ((R.5))$$

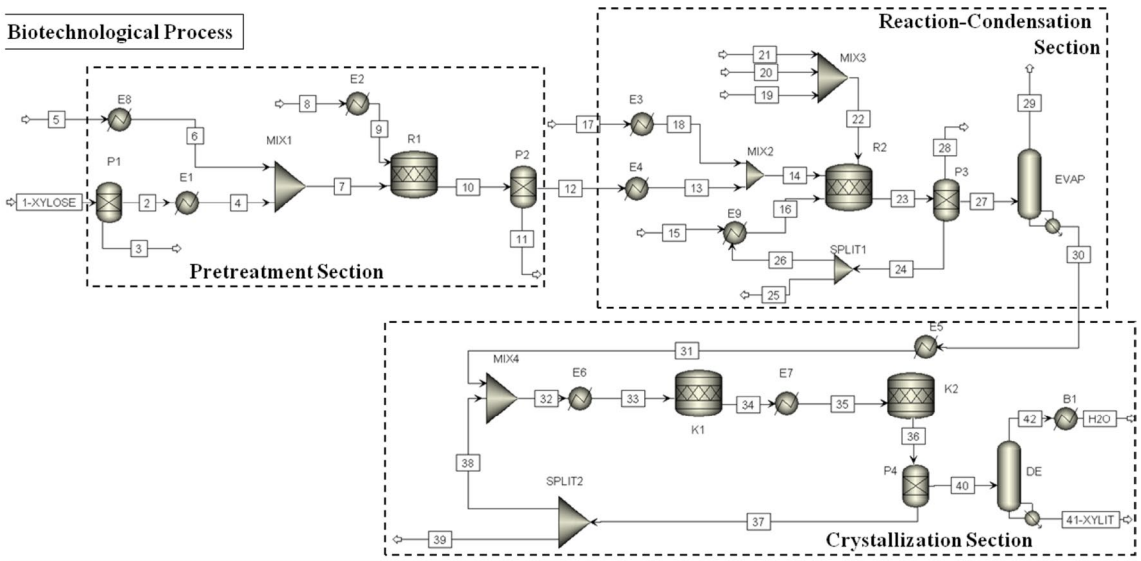

Fig. 6 Aspen flowsheet: Biochemical Xylitol Production

Metabolic Activity:

$$C_6H_{12}O_6 + 3O_2 + 0.6NH_3 + 3H_2 \leftrightarrow 3CH_{1.8}O_{0.5}N_{0.2} + 3CO_2 + 4.5H_2O \quad ((R.6))$$

The crystallization follows a design pattern identical to the catalytic process.

Integration and Path Selection

Both processes demonstrate significant needs for heating and cooling (mainly for evaporation and crystallization). The water use is also significant suggesting options for water re-use and recycle. Process integration should address options within each separate process as well as options to integrate each process with other biorefinery paths (background process). In our case, the background process is the CIMV organosolv biorefinery. Additional paths include the production stages of intermediates, namely the production stages of lignin, C6 and C5 sugars. Process integration is able to curtail haphazard search with simulation experiments, also to offer insights about the potential to combine production processes with each other. Alongside the use of the flowsheeting models presented earlier, the work is required to involve conceptual tools (thermodynamic models, GCCs, water profiles etc.) that may take the form of graphical or mathematical tools [1, 51].

The GCC of the background process (CIMV process™) is shown in Fig. 7. The GCC relates to a threshold problem and accounts for a heat sink of 18 MW. There is an energy pocket between 60 and 80 °C indicating the CIMV bears the potential to integrate with another sink only across the particular interval. In the remaining sections the discussion is intended to review each process first separately and then, subsequently, with respect to the background process.

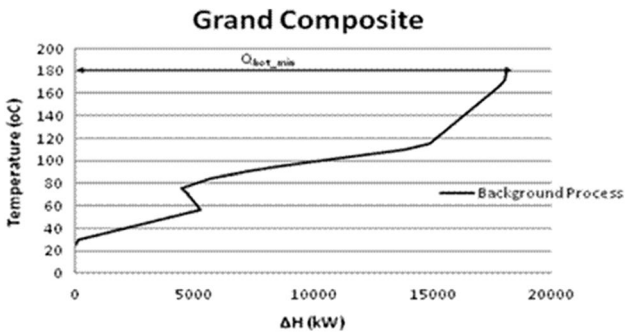

Fig. 7 Grand Composite Curve: CIMV Process ™ (permission CIMV)

Catalytic Process

Basic integration: The process streams are shown on Table 1 and result to the GCC presented in Fig. 8. The pinch is located at 20 °C and the energy use includes 1280 kW hot (T > 25 °C) and 30 kW (T < 10 °C) cold utilities. Energy requirements for cold utilities are lower but expensive. In reference to the flowsheet shown in Fig. 4, integration saves 18% of the total energy use. The operating temperature of the dryer (refs to DE in Fig. 4) is allowed to vary provided that it remains below 105 °C (soft constrain). According to its GCC, the process is almost a heat sink (as is the case of the background process). Without a need for simulation studies, as the energy input is required above 25 °C, it is clear that integration with the background process does not promise any benefits.

Process modifications: The process evaporator brings forward an additional stream (Stream 28, Table 2) that flows at 3,625 kg/h and pressure 0.6 bar. The stream is cooled from 89 to 15 °C (2,611 kW) subsequently condensing to water. Integration with the process streams (e.g. GCC of Fig. 8) is hardly promising as the temperatures cross the pinch, eventually resulting to the GCC of

Table 1 Stream Properties for the Heat Integration of the Chemical Process

Stream	Type	T_{in} (°C)	T_{target} (°C)	CP (kW/°C)
4	Cold	15	87	2.6
11	Cold	76	95	22.1
9	Cold	15	87	0.1
13 + 22	Cold	15	95	0.0
17	Cold	89	100	83.7
15	Cold	15	95	0.1
20	Hot	100	80	6.7
29	Hot	109	8	1.8

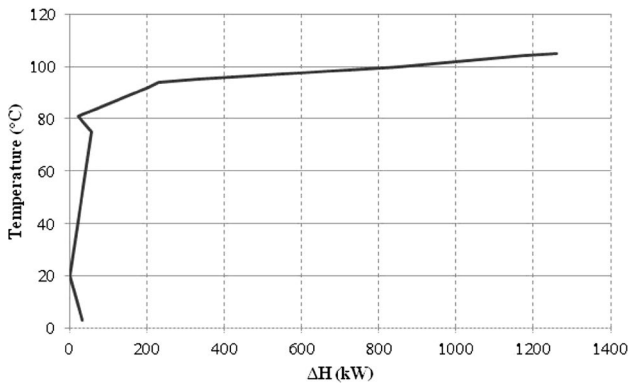

Fig. 8 Grand Composite Curve: catalytic production

Table 2 Additional Stream for the Heat Integration

Stream	Type	T_{in} (°C)	T_{target} (°C)	CP (kW/K)
28	Hot	89	15	35.3

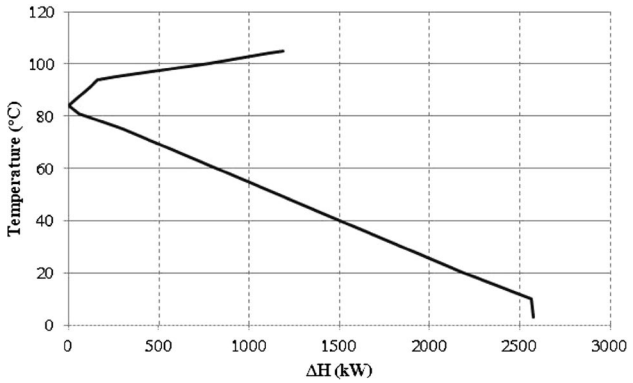

Fig. 9 Grand Composite Curve: catalytic production (water recycle)

Table 3 Hot and Cold Streams of the Biochemical Process

Stream	Type	T_{in} (°C)	T_{target} (°C)	CP (kW/K)
5	Cold	15	25	0.1
8	Cold	15	25	1.7
17	Cold	15	30	40.5
12	Cold	25	30	5.0
15	Cold	15	30	0.0
2	Hot	87	25	4.8
30	Hot	104	15	1.6

Fig. 9. The pinch is raised at 85 °C and the energy use is improved only slightly (1,193 kW hot; 2,559 kW cold), essentially exploiting 3% of the energy available by the process evaporation. However, the integration with the background process could exploit 100% of this energy. Without a need for simulation studies, one could point that, whereas process integration is not promising within the scope of the process, it is entirely justified in the context of the biorefinery. Indeed, evaporation could be extended producing better quality product at no cost.

Biochemical Process

This analysis illustrates the scope to save energy in pilots of continuous production. Process streams are shown on Table 3, and they yield the GCC of Fig. 10. The pinch is located at 20 °C; the energy input is 228 kW (>25 °C) and the energy output 16 kW (<10 °C). As the GCC features an

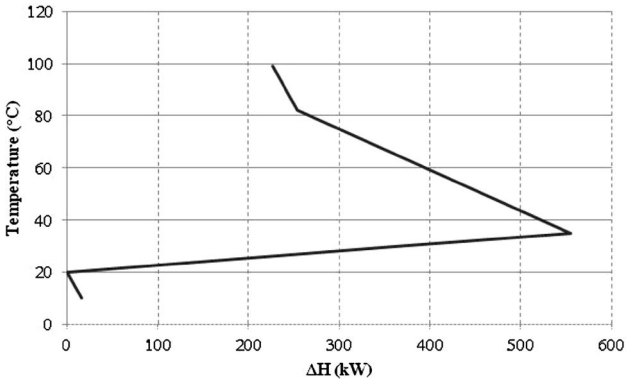

Fig. 10 Grand composite curve: biochemical process (basic case)

energy pocket above the pinch, energy input may become available at lower temperatures (<84 °C). Unlike the case of the catalytic path, the evaporation (energy requirements 27.6 kW) should rather be integrated reducing the total energy use to 21 kW (i.e. by 24%). Indeed, there is scope to even increase the evaporator condensate (a hot stream to become hotter) by recycling water.

The case featuring the recycle is shown in Fig. 11. Unit E3 preheats the fresh water (Stream 17) and the combined stream (recycle and Stream 17) makes the new stream M. The case of a small recycle (0.8%) is presented on Table 4 (M = M1). The recycle conserves 314 kg/h of fresh water while saving energy. The new GCC is presented in Fig. 12. The GGC indicates less energy input (25 kW, reduction 89%) whereas the pinch location remains the same. According to the GCC, and as the evaporator was possible to integrate within the process, further integration with the background process does not promise benefits.

Water recycle, energy and water integration. The need to save water requires larger recycles of water (that will apparently alter the GCC and the scope for energy integration). Let us set the case by recycling 90% of water (M = M2). The properties of M2 are shown on Table 5. The new GCC is shown in Fig. 13. It accounts for a threshold problem (Pinch at 100 °C) depending entirely on cooling (25 kW, T < 94 °C). With the introduction of the large recycle, the process is transformed from an almost balanced system into an energy source. In the context of the particular process, the integration of recycles is only partially justified. However, as the process is an energy source there is scope to integrate with the background process (energy sink). The biochemical process could save the energy used from 80 to 60 °C (see Fig. 7) through process-to-process integration (e.g. with the background process) that reduces energy requirements to 20,085 kW.

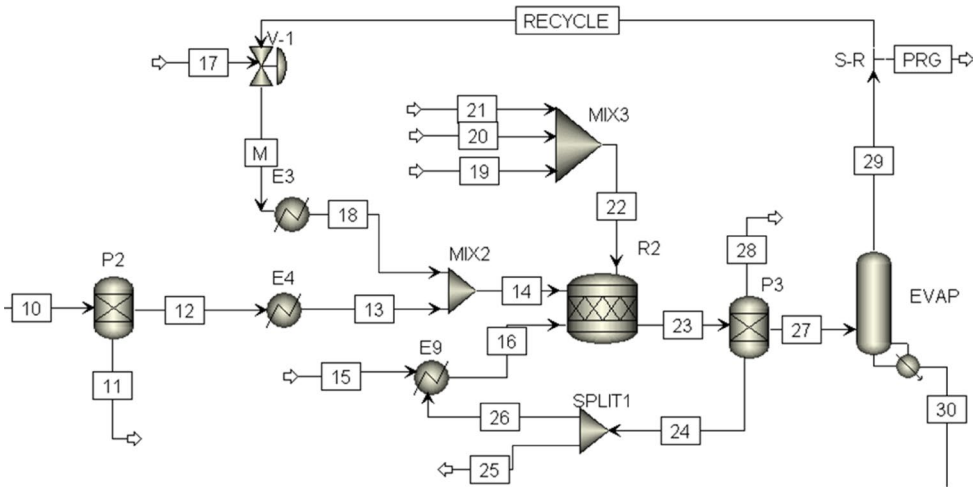

Fig. 11 Simulation of the stream 29-recycle

Table 4 Properties of stream M1

Stream	Type	T_{in} (°C)	T_{target} (°C)	CP (kW/K)
M = M1	Cold	21	30	37.9

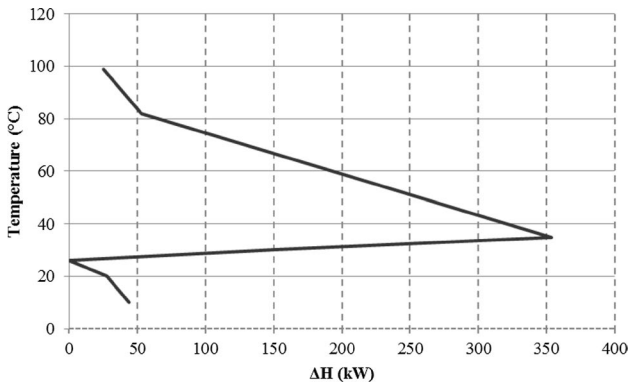

Fig. 12 Grand Composite Curve: biochemical process (0.8% water recycle)

Table 5 Properties of Stream M2

Stream	Type	T_{in} (°C)	T_{target} (°C)	CP (kW/K)
M = M2	Hot	94	30	383.8

Integration Summary

Table 6 summarizes and compares results for the two production paths. The results indicate similarities but also several tradeoffs between the two processes. Results are better understood using the conceptual representations selected for analysis, namely the GCCs for the paths and the GCC of the background process. One should note that simulators

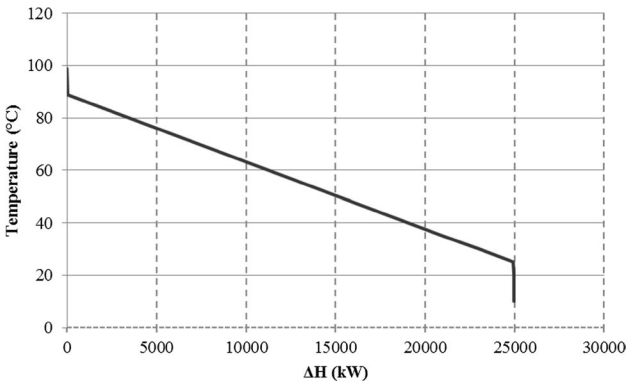

Fig. 13 Grand Composite Curve: biochemical production (90% water recycle)

regularly produce such curves but they do not suggest any ways to modify them. The integration benefits have been primarily in modifying the curves.

Where C% = percentage % of conservation of the cooling needs of the streams.

T% = percentage % of conservation of the heating needs of the streams.

A quick browse of the GCCs superficially suggests that there is limited scope for integration. However, results prove very different as process modifications are introduced. The catalytic process requires additional energy (5 times higher than the biochemical process) due to its high reactor temperatures. Process modifications offer a limited scope to reduce its energy needs but process-to-process integration renders energy-free evaporation. However, the integration of the catalytic process with the background process does not render benefits other those of evaporation. Co-location with the CIMV process may not be necessary.

Table 6 Summarizing Results Regarding the Heat Integration in Every Scenario & Case

Process	T_{pinch} (°C)	Qc_{min} (kW)	Qh_{min} (kW)	C%	T%
Catalytic	20	30	1,280	91	20
Water recycle	84	2,559	1,193	13	24
Biochemical	20	16	228	96	65
Water recycle (0.8%)	25	50	25	89	94
Water recycle (90%)	99	25,085	0	0.2	100

The integration of the evaporation proves particularly promising for the biochemical path. In that case, the integration actually 'invites' the additional use of energy (e.g. free increase in the evaporation load). One possible way would be to recycle (and save) water. Slight increases of recycles are nicely accommodated enhancing integration and reducing treatment costs. Once recycles increase, the process essentially converts from heat source (no recycles) into a sink (large recycles). In this case, the analysis invites further integration beyond the process, namely integration with the background process (e.g. the organosolv process). Accordingly, co-location with the CIMV process is highly recommended.

Economic Evaluation

The paper compares two different methods for costing: a short-cut method that uses basic process information and a more elaborate one that reviews process equipment from Aspen flowsheets that were presented earlier. Tsagkari et al. [52] reviewed cost methods for biorefineries comparing cost models that involve power law estimates, cost factors, significant process steps (e.g. Taylor methods), and thermodynamics (Lange models). The study pointed to several limitations of existing methods and recommended the approach by Lange [53] as the most reliable. Accordingly, the Lange method was selected to estimate capital investment cost (as a short-cut method) results are compared with detailed calculations using the Aspen flowsheets. The analysis analyzed the plant profitability using the net present value (NPV) and payback period (PBP). Prices referred to million € (MM€) in 2014 and are updated using inflation indicators from the chemical engineering plant cost index (CEPCI) [54]. United states dollars (USD $) are converted into euros (€) according to the 2014 year average exchange range [55].

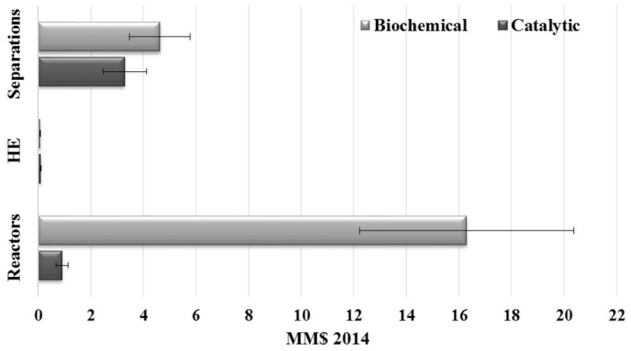

Fig. 14 Equipment cost summary

Capital Cost Estimation

Shortcut Costing

Lange [53] proposed a method to calculate the manufacturing cost based on the lower heating values (LHV) of the components involved (Eq. 1).

$$\text{Investment}\left[\text{MM\$ 1993}\right] = 3.0\,(\text{energy losses [MW]})^{0.84} \quad (1)$$

$$\text{Energy losses} = \text{LHV(feed} + \text{fuel)} - \text{LHV(product)} \quad (2)$$

In Eq. 2, LHV (feed + fuel) is the lower heating value of all feed and fuel streams entering the process; LHV(product) is the lower heating value of the existing products. The method is identified as Class 5 (e.g. accuracy range between −50 and +100%) [56].

The LHV is based on thermodynamic calculations from commercial databases (provided the components were available) and, alternatively, by shortcut models of the form [57].

$$Q\,[\text{Btu/lb}] = 146.58\,C + 568.78\,H + 29.4\,S - 6.58\,\text{Ash} - 51.53\,(N + O) \quad (3)$$

Equation 3 has a marginal error ±15%, and is consistent with the Class 5 accuracy expected by the method.

The manufacturing cost of the catalytic process is estimated at 6.65MM€ and for the biochemical process at 6.57MM€. The LHV calculations for the feed and products are presented in Table 12 in the Appendix.

Detailed Costing

Costing was based on the process flowsheets developed in Aspen Plus. It could be considered as Class 3 [57]. Equipment cost uses correlations from the literature [58, 59] and calculation details are presented on at Tables 13, 14, 15, 16

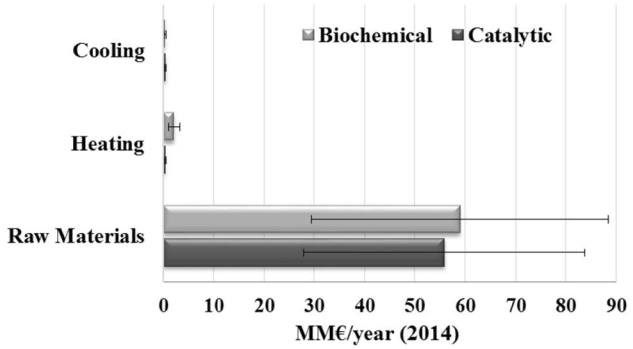

Fig. 15 Utilities & Raw Materials Cost

in the Appendix. For the catalytic process, the equipment cost is estimated at 4.27MM€; for the biochemical it is 20.97MM€. The difference relates to the cost of reactors as illustrated on Fig. 14.

Total Investment Cost Estimation

Non-integrated Processes

- Raw Materials & Utilities Cost

The cost of raw materials is presented on Table 17 in the Appendix and includes the catalyst and the enzyme cultivation cost. Utilities include steam at 7.9 bar, cooling water at 15 °C (T < 25 °C), and refrigerants. The price of raw materials and products is assumed to be the average bulk price found on different commercial sites, with uncertainty ± 50%. Figure 15 summarizes cost calculations for the catalytic and biochemical production.

The total cost for raw materials and utilities (without electricity) is 56.60MM€/year for the catalytic path and 61.41MM€/year for the biochemical. The cost for the cooling and raw materials is similar; heating is six times higher in the biochemical process.

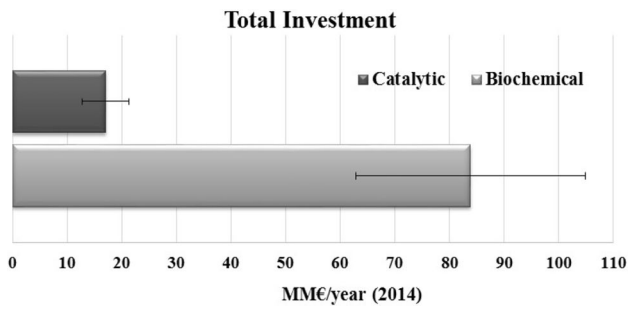

Fig. 16 Cost of total investment

Table 7 Catalytic process costs versus integrated scenarios

Catalytic				
MM€/year	Utilities & raw materials	Total product cost	NPV	PBP
Non-Integrated	56.60	61.72	74.4	1.1
Heat Integration	56.18	60.86	77.6	1.1
Water Recycle	56.45	61.44	75.5	1.1

- Total Investment Cost

Direct and indirect costs are presented on Table 18 in the Appendix. They estimated at 17.08MM€ and 83.88MM€ for the catalytic and the biochemical process respectively. Figure 16 summarizes the results.

The analysis calculates fixed and variable costs following standard procedures [57]; depreciation is calculated separately and assumed flat over 10 years (tax index is 40%). The price of xylitol is assumed at 2.5 €/kg and that of xylose at 1.5 €/kg. NPV and PBP are 74.4 and 1.1 respectively for the catalytic process; they are −59.8 and 21.4 for the biochemical path.

Integrated Processes

The section assesses the impact of integration in economic terms. The scenarios of Table 6 suggested savings in utilities and process water, now translated into cost. Tables 7 and 8 summarize the results for the catalytic and the biochemical process. In the catalytic process, the best integration scenario saves 0.86MM€/year and improves the NPV slightly.

In the case of biochemical process, best integration scenario (utility savings plus water savings) yields cost reductions to 4.7 MM€/year improving NPV by 17.6 points (28%) payback time by 9 years (reduction by 41%).

Sensitivity Analysis

A sensitivity analysis ranges the price of bulk xylitol from 1 to 4 €/kg in order to estimate the impact of price

Table 8 Biochemical process costs vs. integrated scenarios

Biochemical				
MM€/year	Utilities & raw materials	Total product cost	NPV	PBP
Non Integrated	61.41	72.42	−59.8	21.4
Heat Integration	59.70	68.92	−46.7	13.9
Water Recycle (0.8%)	59.12	67.88	−42.9	12.6
Water Recycle (90%)	59.11	67.69	−42.2	12.4

Table 9 Investment Index vs. Xylitol price

Xylose Price	1.5 €/kg							
Xylitol Price	1 €/kg		2 €/kg		3 €/kg		4 €/kg	
	NPV	PBP	NPV	PBP	NPV	PBP	NPV	PBP
Catalytic	−109.9	−1.1	13.0	3.5	135.9	0.7	258.8	0.4
Biochemical	−218.3	−3.8	−112.6	−17.9	−7.0	6.7	98.7	2.8

uncertainty. Changes in the NPV and PBP are presented on Table 9. The break-even price for xylitol is 1.76 €/kg (catalytic) and 2.28 €/kg (biochemical). By a similar token, xylitol prices yield positive NPV at 1.90 and 3.07 €/kg for the catalytic and the biochemical processes.

Using process-to-process integration the break-even prices are reduced for two reasons: (a) offering low competitive prices for xylitol, and (b) benefitting from integration. Xylitol production can be benefitted by a low xylose price at 0.5–1.0 €/kg. Figure 17 illustrates the break-even price of xylitol as a function of xylose (0.5–5 €/kg) and so that to ensure a positive NPV. The lowest points correspond to 0.83 €/kg (catalytic) and 1.83 €/kg (biochemical process).

Table 10 shows the impact of xylose price on process economics.

Integration suggests that utilities can be decreased from 10 to 100%. Figure 18 shows small benefits for the catalytic process (1.90 €/kg to 1.88 €/kg) and higher in the biochemical (3.07 €/kg to 2.92 €/kg; reduction at around 4.9%).

Table 11 highlights reductions in the PBP for fixed prices of feedstock and products.

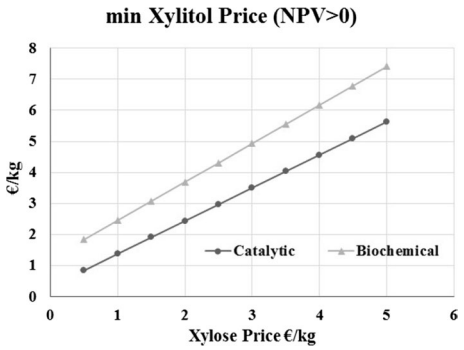

Fig. 17 Minimum Xylitol price vs. Xylose price

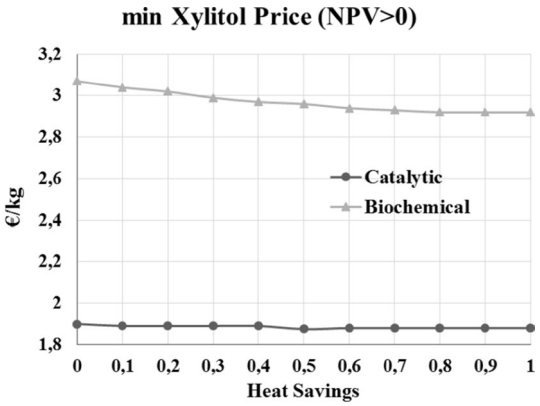

Fig. 18 Minimum Xylitol price versus heat savings

Conclusion

The paper illustrates the significant role of process integration in developing the value chains of a biorefinery. The conventional conceptual tools (GCCs, CCs, TSA plots) are hardly useful to match hot and cold streams. Instead, they are used to suggest modifications, new

Table 11 PBP vs. heat savings

Xylose price	1.5 €/kg	
	Catalytic	Biochemical
Xylitol price	1.90 €/kg	3.07 €/kg
Heat savings%	PBP	
0	5.9	6.1
30	5.5	5.6
60	5.3	5.3
100	5.1	5.1

Table 10 Investment Index vs. Xylose price

Xylitol Price	2.5 €/kg							
Xylose Price	0.5 €/kg		1 €/kg		2 €/kg		3 €/kg	
	NPV	PBP	NPV	PBP	NPV	PBP	NPV	PBP
Catalytic	205.4	0.5	139.9	0.7	9.0	4.0	−122.0	−1.0
Biochemical	71.1	3.3	5.7	5.8	−125.3	−12.5	−256.2	−3.0

process units and to modify the process flowsheet. Process integration proves a life-line for the biochemical path to xylitol guiding to modifications in water treatment and water re-use. Cost calculations have validated these findings. They also confirmed that conventional short-cut cost models should be used only with caution. The two processing paths to xylitol prove quite competitive: the catalytic path yields 0.85 kg xylitol/kg xylose and the biochemical 0.73. The economic evaluation favors the catalytic path but the comparative advantage may be countered by terms of safety, storage, and the use of hydrogen. Sensitivity analysis illustrated the range of changes in break-even prices as a result of variations in the price of feedstocks and products. In general, as this sort of analysis has to be repeated over numerous scenarios and possible products, new conceptual tools and systems technology are needed to scale up the research.

Acknowledgements Financial support from the Consortium of Marie Curie project RENESENG (FP7-607415) is gratefully acknowledged. The authors would also like to thank Marilyn Wiebe and all the people working for the BIOCORE Project (FP7-241566), for their collaboration and excellent communication.

Appendix

See Tables 12, 13, 14, 15, 16, 17 and 18.

Table 12 Shortcut calculations

Catalytic Process				
Components	Mass flow (kg/hr)	LHV (MJ/kg)	LHV (MW)	
Input (feed)				
Xylose	4130.18	14.25	16.35	
		LHVin	16.35	
Components	Mass flow (kg/hr)		LHV (MJ/kg)	LHV (MW)
Output (products)				
Xylose	195.90		14.25	-
Xylitol (Product)	3,972.45		16.88	18.63
Xylulose	1.03		14.25	-
Arabinose	9.41		14.25	-
			LHVout	18.63
ΔH_{LHV} (MW)	Equipment cost (M$ 1993)		Equipment cost (M€ 2014)	
2.28	5.99		6.65	
Biochemical process				
Components	Mass flow (kg/hr)		LHV (MJ/kg)	LHV (MW)
Input (feed)				
Xylose	4,130.18		14.25	16.35
Glucose	400.00		17.10	1.90
Yeast	1.30		18.74	0.01
			LHVin	18.26
Components	Mass flow (kg/hr)		LHV (MJ/kg)	LHV (MW)
Output (products)				
Xylitol (product)	3,413.98		16.88	16.01
Yeast	388.73		18.74	-
Xylose	210.70		14.25	-
Glucose	4.00		17.10	-
			LHVout	16.01
ΔH_{LHV} (MW)	Equipment cost (MM$ 1993)		Equipment cost (MM€ 2014)	
2.25	5.92		6.57	

Table 13 Cost estimation of the heat exchangers in the catalytic process

Catalytic Process- Heat Exchangers						
Equipment	Description	ΔTm	U [W/(m^{2}K)]	Q (W)	A (m^2)	Cost ($ 1980)
E1	Double pipe, stainless steel 316	54.2	750	189,854	4.7	3231
E2	Double pipe, stainless steel 316	58.8	150	6935	0.8	1795
E3	Shell and tube, type U-tube, stainless steel 316	28.4	750	428,294	20.1	11,425
E4	Double pipe, stainless steel 316	58.1	150	9118	1.1	1982
E5	Double pipe, stainless steel 316	25.4	750	25	0.2	1042
E6	Shell and tube, type U-tube, stainless steel 316	22.4	500	133,187	11.9	8394
E7	shell and tube, type U-tube, stainless steel 316	54.3	400	180,035	8.3	6933
E10	Shell and tube, type U-tube, stainless steel 316	22.4	750	936,828	55.8	22,871
Total cost ($1980)						57,673
Total cost (€2014)						85,607

Table 14 Total equipment cost estimation of the catalytic process

Catalytic process-total equipment						
Equipment	Type	Description	#	Cost ($)	Total Cost ($)	Cost € (2014)
R1 ($2002)	Continuous	Volume 1 m^3,with mantle and agitation, stainless steel, pressure endurance 3 bar	1	20,000	20,000	21,958
R2 ($2002)	Continuous	Volume 57.6 m^3, with mantle and agitation, stainless steel, pressure endurance 60 bar	1	800,000	800,000	878,305
EVAP ($1980)	Evaporator	Long tube, U = 900 [W/(m^2 K)], ΔTm = 13.5, Q = 2.4 MW, A(m^2) = 197.1, stainless steel	1	242,038	242,038	359,270
DE ($1980)	Dryer	Spray dryer, stainless steel 316	1	659,034	659,034	978,239
K ($1980)	Crystallizer	External forced circulation, stainless steel 304	1	751,265	751,265	1,115,143
P1 ($2002)	Chromatographic separation-Ion exchange resigns –activated carbon column	Vertical cylindrical container, stainless steel, volume = 5.2 m^3, diameter = 1.3 m, height = 3.9 m	3	96,772	290,315	318,731
P2 ($1980)	Filter	Sieve, surface 1 m^2	1	12,596	12,596	18,697
P3 ($1980)	Centrifugal	Stainless steel	1	141,472	141,472	209,994
P4(2002)	Ion exchange resign—activated carbon column	Vertical cylindrical container, stainless steel, volume = 7.2 m^3, diameter = 1.5 m, height = 4.1 m	2	122,629	245,258	269,264
P5 ($1980)	Filter	Rotary vacuum disk, surface = 1 m^2	1	8832	8,832	13,110
E($1980)	Heat exchangers	Table 13	–	–	57,673	85,607
Total equipment cost (€2014)						4,268,318

Table 15 Cost estimation of the heat exchangers in the biochemical process

Biochemical process—heat exchangers						
Equipment	Description	ΔTm	U [W/(m^2 K)]	Q (W)	A (m^2)	Cost $ (1980)
E1	Shell and tube, type U-tube, stainless steel 316	40.8	500	295,373	14.5	9380
E2	Double pipe, stainless steel 316	23.7	750	16,721	0.9	1912
E3	Shell and tube, type U-tube, stainless steel 316	25.2	750	608,105	32.1	15,452
E4	Double pipe, stainless steel 316	15.4	750	24,780	2.1	2518
E5	Shell and tube, type U-tube, stainless steel 316	52.8	400	154,939	7.3	6524
E8	Double pipe, stainless steel 316	39.6	750	1278	0.2	1042
E9	Double pipe, stainless steel 316	23.7	750	8	0.2	1042
Total cost ($1980)						37,870
Total cost (€2014)						56,212

Table 16 Total equipment cost estimation of the biochemical process

Biochemical process- total equipment						
Equipment	Type	Description	#	Cost $	Total Cost $	Cost € (2014)
R1 ($2002)	Continuous flow reactor	Volume 1 m^3,with mantle and agitation, stainless steel, pressure endurance 3 bar	1	20,000	20,000	21,958
R2 ($2002)	Batch reactor	Volume 50 m^3 (total volume 3900 m^3), with mantle and agitation, stainless steel, pressure endurance 3 bar	78	190,000	14,820,000	16,270,599
EVAP ($1980)	Evaporator	Long tube, U = 900 W/(m^2 K), ΔTm = 25.6, Q = 27.6 MW, A = 1,197.6 m^2, stainless steel	1	1,122,137	1,122,137	1,665,648
DE ($1980)	Dryer	Spray dryer, stainless steel 316	1	618,472	618,472	918,031
K ($1980)	Crystallizer	External forced circulation, stainless steel 304	1	713,385	713,385	1,058,915
P1 ($2002)	Chromatographic separation-ion exchange resins—activated carbon column	Vertical cylindrical container, stainless steel, volume = 5.2 m^3, diameter = 1.3 m, height = 3.9 m	3	96,772	290,316	318,732
P2 ($1980)	Filter	Sieve, surface 1 m^2	1	12,596	12,596	18,697
P3 ($1980)	Filter	Sieve, surface 2 m^2	1	18,958	18,958	28,140
P4 ($2002)	Activated carbon column	Vertical cylindrical container, stainless steel, volume = 44.6 m^3, diameter = 2.5 m, height = 9.1 m	1	545,830	545,830	599,256
P5 ($1980)	Filter	Rotary vacuum disk, surface = 1 m^2	1	8832	8832	13,110
E($1980)	Heat exchangers	Table 15	–	–	37,870	56,212
Total Equipment Cost (€2014)					20,969,298	

Table 17 Raw materials and utilities cost

Raw materials and utilities cost							
Catalytic process				Biochemical process			
Utilities							
Heating steam	4.40$/tn (2002)						
Equipment	[KW]	Steam tn/hr	Cost 2002 ($/hr)	Equipment	[KW]	Steam tn/hr	Cost 2002 ($/hr)
E1	189.85	0.33	1.47	E2	16.72	0.03	0.13
E2	6.94	0.01	0.05	E3	608.11	1.07	4.71
E3	428.29	0.75	3.31	E4	24.78	0.04	0.19
E4	9.12	0.02	0.07	E7	147.85	0.26	1.14
E5	0.03	0.00	0.00	E8	1.28	0.00	0.01
E9	164.52	0.29	1.27	E9	0.01	0.00	0.00
E10	936.83	1.65	7.25	EVAP	27600.00	48.55	213.62
EVAP	2400.00	4.22	18.58	DE	21.00	0.04	0.16
DE	24.00	0.04	0.19	R1	598.76	1.05	4.63
R1	515.92	0.91	3.99	K2	0.14	0.00	0.00
K2	0.15	0.00	0.00				
Total Heating		€/hr (2014)	39.73			€/hr (2014)	246.58
Cooling water	0.08$/tn (2002) KW	Water (tn/h)	Cost 2002 ($/hr)		KW	Water (tn/h)	Cost 2002 ($/hr)
E6	133.19	4.58	0.37	E1	295.37	10.17	0.81
R2	2895.43	99.68	7.97	R2	2591.87	89.23	7.14
		€/hr (2014)	9.16			€/hr (2014)	8.73
Cooling to 5 °C	20$/GJ (2002) KW	GJ/hr	Cost 2002 ($/hr)		KW	GJ/hr	Cost 2002 ($/hr)
E7	180.04	0.65	12.96	E5	154.94	0.56	11.16
		€/hr (2014)	14.23			€/hr (2014)	12.25
Cooling to -20 °C	32$/GJ (2002) KW	GJ/hr	Cost 2002 ($/hr)		KW	GJ/hr	Cost 2002 ($/hr)
E8	164.30	0.59	18.93	E6	147.09	0.53	16.94
K1	1.87	0.01	0.22	K1	1.70	0.01	0.20
		€/hr (2014)	21.02			€/hr (2014)	18.82
Total cooling	€/hr (2014)		44.41		Total €/hr (2014)		39.80

Table 17 (continued)

Raw materials							
	Quantity (kg/hr)	Unit price €/kg (2014)	Cost (M€/hr)		Quantity kg/hr	Unit price €/kg (2014)	Cost (M€/hr)
Xylose	4130.18	1.50	6.20	Xylose	4130.18	1.50	6.20
Water	2293.62	0.54 €/tn	0.001	Water	381538.90	0.54 $/tn	0.21
Calcium Hydroxide	169.34	0.11	0.02	Calcium Hydroxide	113.61	0.11	0.01
Hydrogen	115.4	1.40 €	0.16	Glucose	400.00	0.80	0.32
Raney Nickel Catalyst	2.00	60.60	0.12	Yeast cultivation cost		0.12 €/hr	
Total Materials	M€/hr		6.50		M€/hr		6.85
Total Utilities& Material Cost		56.60 MM€/year		Total Utilities& Material Cost		61.41 MM€/year	

Hours per year: 8600

Table 18 Calculation of the total fixed investment

Calculation of the Total Fixed Investment			
Individual costs	Percentage of the total investment (%)	Estimated cost (MM€2014)	
		Catalytic	Biochemical
Direct costs			
Equipment	25	4.27	20.97
Equipment's installation	9	1.54	7.55
Instrumentation and control	8	1.37	6.71
Pipes	7	1.20	5.87
Electrical costs	4	0.68	3.36
Buildings	6	1.02	5.03
Improvements to land	2	0.34	1.68
Facilities for services	12	2.05	10.07
Land	1	0.17	0.84
Indirect costs			
Engineering services and supervision	8	1.37	6.71
Construction costs	10	1.71	8.39
Legal expenses	2	0.34	1.68
Contractor's fee	2	0.34	1.68
Unpredictable	5	0.85	4.19
Summary	100		
Total fixed investment (MM€2014)		17.08	83.88

References

1. Smith, R.: Chemical Process Design and Integration. Willey, Oxford (2014)
2. Smith, R., Jobson, M., Chen, L.: Recent development in the retrofit of heat exchanger networks. Appl. Therm. Eng. **30**, 2281–2289 (2010)
3. Gadalla, M., Jobson, M., Smith, R.: Optimization of existing heat-integrated refinery distillation systems, Chem. Eng. Res. Des. **81**, 147–152 (2003).
4. Gunaratnam, M, Alva-Argez, A., Kokossis, A.C., Kim, J.K., Smith, R.: Automated design of total water systems, Ind. & Eng. Chem. Res. **44**, 588–599 (2005).
5. Nikolakopoulos, A., Karagiannakis, P., Galanis, A., Kokossis, A.C.: A water saving methodology for the efficient development of biorefineries, ESCAPE 22, Elsevier, London, UK, 6–10 (2011).
6. Wang, Y.P., Smith, R.: Wastewater Minimisation. Chem Eng Sci. **49**, 981–1006 (1994)
7. Alva-Argaez, A., Kokossis, A.C., Smith, R.: Wastewater minimization of industrial systems using an integrated approach, Comp. Chem. Eng. **22**, 741–744 (1998)
8. Alva-Argaez, A., Vallianatos, A., Kokossis, A.C.: A multicontaminant transshipment model for mass exchange networks and wastewater minimization problems. Comp. Chem. Eng. **23**, 1439–1453 (1999)

9. Stefanakis, M.E., Pyrgakis, K., Mountraki, A.D., Kokossis, A.C.: The Total Site Approach as a synthesis tool for the selection of valorization paths in lignocellulosic biorefineries, ESCAPE 23, Lappeenranta, Finland, (2013)
10. El-Halwagi, M.M.: Process Integration. Academic Press, San Diego (2006)
11. Tsoka, C., Johns, W.R., Linke, P., Kokossis, A.C. A.: Towards sustainability and green chemical engineering: tools and technology requirements. Green Chem. **6**(8), 401–406 (2004)
12. Kokossis, A.C., Yang, A.: On the use of systems technologies and a systematic approach for the synthesis and the design of future biorefineries. Comp. Chem. Eng. **34**(9), 1397–1405 (2010)
13. Mountraki, A., Nikolakopoulos, A., Benjelloun- Mlayah, B., Kokossis, A.C.: BIOCORE—A systems integration paradigm in the real-life development of a lignocellulosic biorefinery. Comp. Chem. Eng.29 1381–1385 (2011)
14. Kokossis, A., Tsakalova, M., Pyrgakis, K.: Design of integrated biorefineries, Comp. Chem. Eng. **81**, 40–56 (2015)
15. Kokossis, A., Yang, A., Tsakalova, M., Lin, T.C.: A systems platform for the optimal synthesis of biomass based manufacturing systems. Comp. Aid. Chem. Eng. **28**, 1105–1110 (2010)
16. Psycha, M., Pyrgakis, K., Kokossis, A.C.: Process design analysis for the valorization and selection of integrated micro-algae biorefineries, Comp. Aid. Chem. Eng. **33**, 1543–1548 (2014)
17. Koufolioulios D., Nikolakopoulos A., Pyrgakis K., Kokossis, A.: A Mathematical Decomposition for the Synthesis and the Application of Total Site Analysis on Multi-product Biorefineries, FOCAPD 2014, Cle Elum, Elsevier, Washington (2014).
18. Stefanakis, M.E., Pyrgakis, K.A., Kokossis, A.C.: Screening and assessing product portfolios in biorefineries: combining total site analysis and process synthesis, Comp. Aid. Chem. Eng. **34**, 621–626 (2014)
19. Tsakalova M., Lin, T.C., Yang, A., Kokossis A.C.: A decision support environment for the high-throughput model-based screening and integration of biomass processing paths, Ind. Crops & Prod. **75**, 103–113 (2015).
20. Mountraki, A.D., Benjelloun Mlayah, B., Kokossis, A.C.: A Study on the Endogenous Symbiosis of First and Second Generation Biorefineries: Towards a Systematic Methodology. ESCAPE 26, June 12–15, Portorož, Slovenia, Elsevier, 385–390 (2016)
21. Mountraki, A., Nikolakopoulos, A., Benjelloun Mlayah, B., Kokossis, A.C.: BIOCORE– A systems integration paradigm in the real-life development of a lignocellulosic biorefinery. ESCAPE 21, May 29-June 1, Chalkidiki Greece, Elsevier, 1381–1385 (2011)
22. Tsakalova, M., Kokossis, A.: On the systematic synthesis screening and integration of real-life biorefineries. In Symposium on Biorefinery for Food, Fuel, and Materials, Wagenigen, The Netherlands. Ton van Boxtel and Marieke Bruins, Wagenigen (2013).
23. Pal, S., Choudhary, V., Kumar, A., Biswas, D., Mondal, A.K., Sahoo, D.K.: Studies on xylitol production by metabolic pathway engineered Debaryomyces hansenii. Biores. Technol. **147**, 449–455 (2013).
24. Fatehi, P., Catalan, L., Cave, G.: Simulation analysis of producing xylitol from hemicelluloses of pre-hydrolysis liquor. Chem. Eng. Res. Des. **92**, 1563–1570 (2014).
25. Lima, T., José, I., Ribeiro, G., Valderez, M.: Biotechnological production of xylitol from lignocellulosic wastes: A review. Process Biochem. **49**, 1779–1789 (2014)
26. Wisniak, J., Hershkowitz, M., Leibowitz, R., and Stein, S.: Hydrogenation of xylose to xylitol. Ind. Eng. Chem. Prod. Res. Dev. **13**(1), 75–79 (1974).
27. Parajó, J.C., Domínguez, H., Domínguez, J.M.: Biotechnological production of xylitol. Part 1: Interest of xylitol and fundamentals of its biosynthesis. Biores. Technol. **65**(3), 191–201 (1998).
28. Aranda-Barradas, J.S., Garibay-Orijel, C., Badillo-Corona, J.A., Salgado-Manjarrez, E.: A stoichiometric analysis of biological xylitol production. Biochem. Eng. J. **50**, 1–9 (2010)
29. Research and Markets: Xylitol - A Global Market Overview, report ID: 2846975. (http://www.researchandmarkets.com/reports/2846975/xylitol-a-global-market-overview) (2014), Accessed June 17 2016.
30. Cheng, K., Wu, J., Lin, J., Zhang, J.: Aerobic and sequential anaerobic fermentation to produce xylitol and ethanol using non-detoxified acid pretreated corncob. Biotechnol. Biofuel **7**(1), 166 (2014).
31. Snelders, J., Dornez, E., Benjelloun-Mlayah, Huijgen, W.J.J., de Wild, P.J., Gosselink, R.J.A., Gerritsma, J., Courtin, C.M.: Biorefining of wheat straw using an acetic and formic acid based organosolv fractionation process. Bioresour. Technol. **156**, 275–282 (2014)
32. Delmas, M.: Vegetal refining and agrochemistry. Chem. Eng. Technol. **31**(5), 792–797 (2008).
33. Briones, V. and Kokossis, A.C.: A new approach for the optimal retrofit of heat exchanger networks. Comp. Chem. Eng. **20** (SUPPL.1), S43–S48 (1996).
34. Mavromatis, S.P. and Kokossis, A.C.: Hardware composites: A new conceptual tool for the analysis and optimisation of steam turbine networks in chemical process industries. Part I: Principles and construction procedure. Chem. Eng. Sci. **53**(7), 1405–1434 (1998).
35. Mavromatis, S.P., Kokossis, A.C.: Conceptual optimisation of utility networks for operational variations - II. Network development and optimisation. Chem. Eng. Sci. **53**(8), 1609–1630 (1998).
36. Tantimuratha, L., Asteris, G., Antonopoulos, D.K., Kokossis, A.C.: A conceptual programming approach for the design of flexible HENs. Comp. Chem. Eng. **25**(4–6), 887–892 (2001)
37. Linke, P., Kokossis, A.: Advanced process systems design technology for pollution prevention and waste treatment. Adv. Env. Res. **8**(2), 229–245 (2004).
38. Mountraki, A.D., Koutsospyros, K.R., Kokossis, A.C.: The Role of Process Integration in Reviewing and Comparing Biorefinery Processing Routes: The Case of Xylitol. Process. Chapter 12, pp, 309–329, Design Strategies for Biomass Conversion Systems, John Wiley & Sons, Inc.,Oxford (2015)
39. Mikkola, J.P., Sjöholm, R., Salmi, T., Mäki-Arvela, P.: Xylose hydrogenation: Kinetic and NMR studies of the reaction mechanisms. Catal. Today. **48**(1), 73–81 (1999)
40. Mikkola, J.P., Vainio, H., Salmi, T., Sjöholm, R., Ollonqvist, T., Väyrynen, J.: Deactivation kinetics of Mo-supported Raney Ni catalyst in the hydrogenation of xylose to xylitol. Appl. Catal., A. **196**(1), 143–155 (2000)
41. Mikkola, J.P., Salmi, T.: Three-phase catalytic hydrogenation of xylose to xylitol—Prolonging the catalyst activity by means of on-line ultrasonic treatment. Catal. Today. **64**(3), 271–277 (2001)
42. Misra, S., Gupta, P., Raghuwanshi, S., Dutt, K., Saxena, R.K.: Comparative study on different strategies involved for xylitol purification from culture media fermented by Candida tropicalis. Sep. Pur. Technol. **78**(3), 266–273 (2011).
43. Yahashi, Y., Horitsu, H., Kawai, K., Suzuki, T., Takamizawa, K.: Production of xylitol from D-xylose by Candida tropicalis: the effect of D-glucose feeding. J. Ferment. Bioeng. **81**(2), 148–152 (1996)
44. Tochampa, W., Sirisansaneeyakul, S., Vanichsriratana, W., Srinophakun, P., Bakker, H. H., Chisti, Y.: A model of xylitol production by the yeast Candida mogii. Bioprocess Biosyst. Eng. **28**(3), 175–183 (2005)

45. Faria, L.F.F., Pereira, N. Jr., Nobrega, R.: Xylitol production from d-xylose in a membrane bioreactor. Desalination. **149**(1), 231–236 (2002)
46. Branco, R.F., Santos, J.C., Murakami, L.Y., et al.: Xylitol production in a bubble column bioreactor: Influence of the aeration rate and immobilized system concentration. Process Biochem. **42**(2), 258–262 (2007)
47. Parajó, J.C., Dominguez, H., Domínguez, J.: Biotechnological production of xylitol. Part 3: Operation in culture media made from lignocellulose hydrolysates. Bioresour. Technol. **66**(1), 25–40 (1998)
48. Nigam, P., Singh, D.: Processes of fermentative production of Xylitol - a sugar substitute. Process Biochem. **30**(2), 117–124 (1995)
49. Silva, S.S., Roberto, I.C., Felipe, M.G., Mancilha, I.M.: Batch fermentation of xylose for xylitol production in stirred tank bioreactor. Process Biochem. **31**(6), 549–553 (1996)
50. Jiang, Z., Wu, P: Pseudo-steady state method on study of xylose hydrogenation in a tricklebed reactor. Catal. Today. **44**(1), 351–356 (1998)
51. Kemp, I.C.: Pinch Analysis and Process Integration: A User Guide on Process Integration for the Efficient Use of Energy. Butterworth-Heinemann, Oxford (2011)
52. Tsagkari, M., Couturier, J.L., Kokossis, A., Dubois, J.L.: Early-stage capital cost estimation of biorefinery processes: a comparative study of heuristic techniques. ChemSusChem. **9**(17), 2284–2297 (2016)
53. Lange J.: Fuels and chemicals manufacturing, guidelines for understanding and minimizing the production costs. Cattech, **5**(2), 82–95 (2001).
54. Compass International, Global Construction Cost and Reference Yearbook, Compass International, Inc, 2016. "http://www.chemengonline.com/pci-home [Online].
55. European Central Bank, https://www.ecb.europa.eu/stats/exchange/eurofxref/html/eurofxref-graph-usd.en.html, Accessed 08 Dec 2016.
56. Christensen P., Dysert L.R.: Cost estimate classification system–as applied in engineering, procurement, and construction for the process industries. AACE International Recommended Practice No. 18R-97 (2016).
57. Mason, D.M., Gandhi K.: Formulas for calculating the heating value of coal and coal char: development, tests and uses. Am Chem. Soc. Div. Fuel Chem. **25**, 235–245 (1980).
58. Peters, M.S., Timmerhaus, K.D., West, R.E.: Plant Design and Economics for Chemical Engineers, 5th edition, McGraw-Hill. Higher Education, New York (2003)
59. Couper, J.R., Penney, W.R., Fair, J.R., Walas, S.M.: Chemical Process Equipment, Selection and Design (Third Edition). Elsevier, USA (2012)